

# A COMPARISON OF VARIOUS BELT TENSION CALCULATION METHODOLOGIES INCLUDING CEMA 6<sup>TH</sup> EDITION

David J. Kruse and Ryan Lemmon

## 1. OVERVIEW

Over the past four decades there have been various international standards developed to determine the power consumption of belt conveyors (DIN, ISO, and CEMA) [1, 2, 3, 4]. Numerous papers have also been published on this topic. Many of these papers are focused on the detailed theoretical calculations required to determine specific power loss components. Other papers have presented field measurements and case studies [5, 6, 7].

The focus on belt conveyor power consumption is no doubt due to the fact that this single value dictates a significant portion of the conveyor design. Pulley design forces, belt ratings, structural loads, and major equipment selection are but a few items based on this value. Furthermore, without accurate steady state power estimates, the dynamic behavior of the system and governing control logic can not be determined.

By investigating and thoroughly understanding each of the major power loss components, the engineer can design safer, more reliable, and more economical conveyor systems. The boundaries of overland conveyor design have not even begun to slow down over the past three decades. The use of new and advanced conveyor technologies continues to push the limits of what was once considered either too risky, or to costly.

The intention of this paper is to discuss the components that constitute the belt conveyor power requirements, and also to show how these components are typically calculated. Many of the basic principles have been known for decades. However, with current computing power, and new software technology, many items which were once considered simple “rule of thumb” or “black box equations” are being investigated in far more detail. Due to the recent release of the CEMA 6<sup>th</sup> edition book (April 2007 revision), the author will particularly focus on these new equations and how they compare to other published information. When possible the equations will be compared with experimental measurements. Finally, several case studies from conveyors around the globe will be compared with the discussed calculation methods.

## 2. INDIVIDUAL TENSION COMPONENTS

The power consumption of a belt conveyor can be calculated by simply multiplying the effective belt tension ( $T_e$ ) at the drives by the conveyor speed ( $P = T_e \cdot V$ ). Since the speed of the conveyor is known (or will be specified) the  $T_e$  tension of the conveyor is all that needs to be determined.

The DIN and ISO calculations methodologies give broad and general guidelines for determining the  $T_e$  tension. These methods are useful for relatively short and simple conveyors. However they also “put the cart in front of the horse” so to speak. The designer has to choose an equivalent friction factor up front ( $T = \mu_e \cdot W_{mb}$ ). Although this factor excludes the material lift, it lumps all other major design items together. A more scientific method to calculate the equivalent friction factor is to break the conveyor into its basic components, and then sum up each of these individual items. The equivalent friction factor is thus the result of conveyor design process, and not the other way around!

The conveyor  $T_e$  tension is typically divided into four major components, with several subcategories of each. These are:

1. Material Components
  - a. Lift ( $T_{ml}$ )
  - b. Acceleration of material at load station ( $T_{ma}$ )
2. Idler Components
  - a. Roll Drag ( $T_{rd}$ )
  - b. Idler Alignment ( $T_{ia}$ )

3. Belt Components
  - a. Rubber Indention ( $T_{ri}$ )
  - b. Belt Flexure ( $T_{bf}$ )
  - c. Material Flexure ( $T_{mf}$ )
4. Mechanical Components
  - a. Drive Assembly (Reducer, Fluid Coupling, etc)
  - b. Pulley Bearing Drag Losses ( $T_{pd}$ )
  - c. Belt Scrapers ( $T_{bs}$ ) & Skirtboard Drag ( $T_{sd}$ )
  - d. Other Minor Mechanical Losses

Summing up the above components results in a total  $T_e$  tension of:

$$T_e = T_{ml} + T_{ma} + T_{rd} + T_{ia} + T_{ri} + T_{bf} + T_{mf} + T_{pd} + T_{bs} + T_{sd}$$

Figure 1 shows the breakdown of power for a flat 1,000 m conveyor transporting coal at 2,500 T/H. As will be shown, different calculation methodologies result in significant differences in individual tension components as well as the total power consumption.

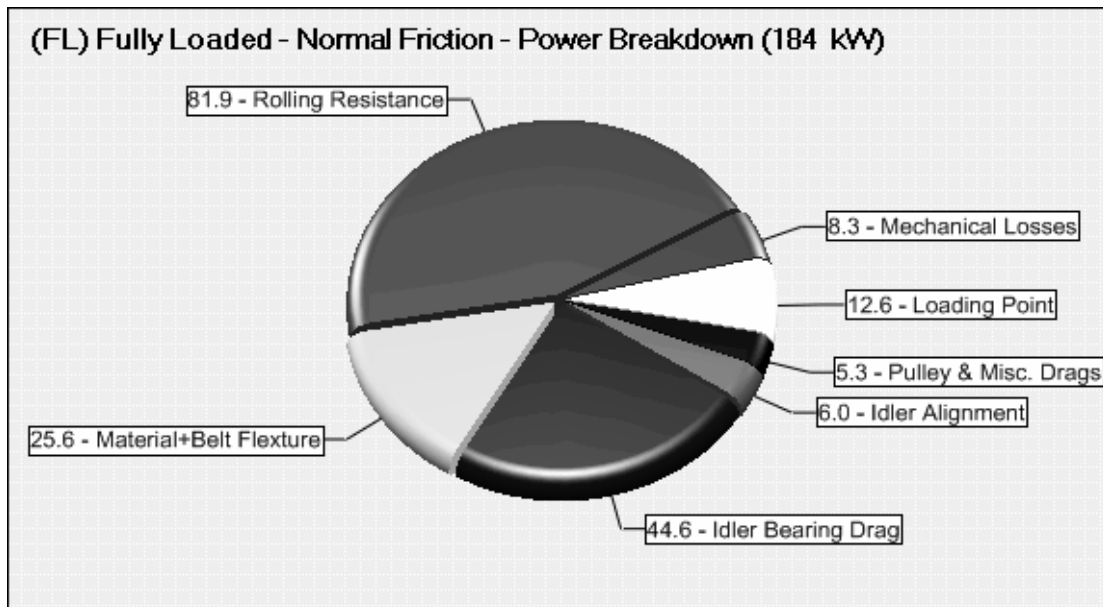


Figure 1 – Power breakdown for a 1,000m flat conveyor

### 3. MATERIAL COMPONENTS

#### 3.1 LIFT

Material lift is perhaps the only tension component which engineers completely agree on the calculation. Furthermore, on many incline (or decline) conveyors this component can represent over 80% of the demand power. The remaining loss components are therefore very small in comparison. Their optimization (while still important) cannot make major contributions to the final power requirements [8].

The tension equation for lift is:

$$T_{ml} = w_m * h$$

Where:

- $w_m$  = material Force per meter N/m)
- $h$  = total height to be lifted (m)

Figure 2 shows the power breakdown for the previous 1,000 m conveyor. However, this time the conveyor has been inclined at 12 degrees. Material lift and mechanical losses now

account for 85% of the power consumption. The remaining 290 kW of power represents only 15% of the total power consumption. This however is still not an insignificant cost when considering the total life of the conveyor. Furthermore, some incline systems may have partially loaded conditions which could dictate the minimum belt safety factor, maximum belt drift time, transfer chute requirements, or other design factors. In these cases the material lift might only represent a small portion of the total power consumption. Thus the remaining components (which were previously minor losses) could in fact still have a significant effect on the design.

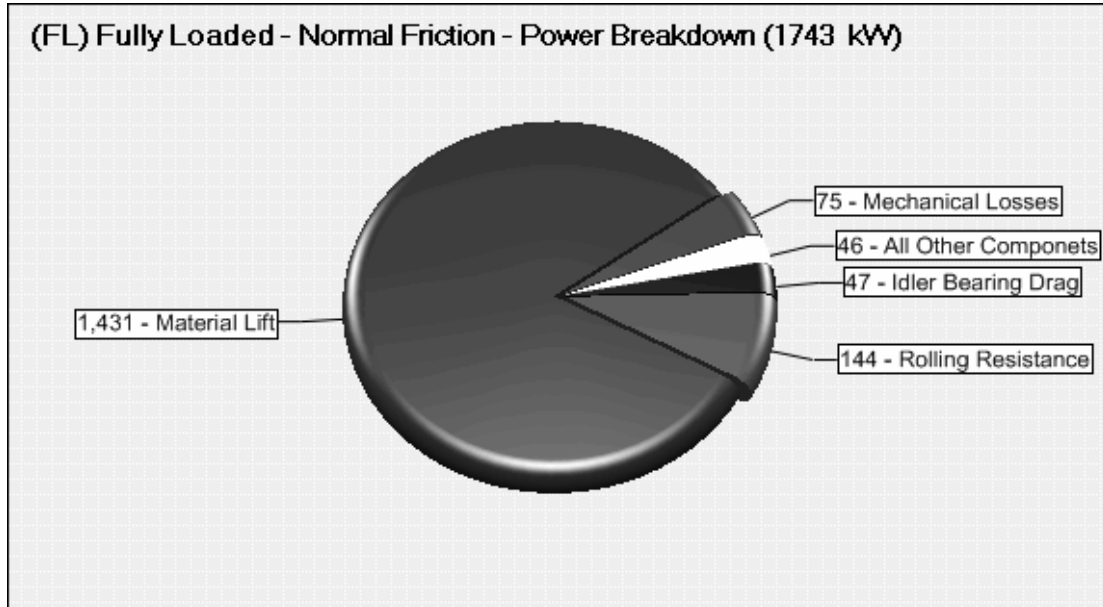


Figure 2 – Power breakdown for a 1,000 m conveyor sloped at 12 degrees

### 3.2 MATERIAL ACCELERATION

The tension component for material acceleration is also widely agreed upon and easy to calculate. As the material leaves the transfer chute it must be accelerated by the belt to full speed. The only point of contention in this calculation becomes the material's initial velocity as it leaves the transfer chute (and in the belt direction). This is often simply taken as zero for a conservative estimate, or the author recommends:

$$V_i = 0.44 * h_c^{0.5} \text{ – Inline Rockbox Design}$$

$$V_i = 1.1 * h_c^{0.5} \text{ – Curved Chute Design}$$

Where:  $h_c$  = material free fall height in chute (m)

The material acceleration is then:

$$T_{ma} = w_m * (V - V_i)^2$$

On high tonnage conveyors which are relatively short (e.g. cross conveyors), this acceleration term can be quite large. This is particularly true if the receiving belt transfer chute is at right angles to the feed and the material has little or no forward velocity.

## 4. IDLERS

### 4.1 SEAL DRAG

At first glance one would consider idler losses to be relatively straightforward to calculate. A single idler can be isolated from all other components and individually tested in a laboratory. However, to date there are still major variations in published idler drag measurements. Furthermore, it is often extremely difficult to get idler manufacturers to publish drag values for their particular components. This is primarily due to the stigma that low drag idlers are superior, which is not necessarily always the case. Of course a low drag idler will result in

lower belt tensions and power consumption, but a proper seal design should NEVER be compromised in exchange for a lower idler drag. After all, a bearing without any seals would result in the lowest idler drag possible. However idler drag would quickly become the least of a clients concerns when idler bearings begin failing at record rates from contamination and corrosion!

The CEMA 5<sup>th</sup> edition calculates the idler drag as a function of the roll diameter, and a global temperature correction factor  $K_t$ . The  $K_t$  factor is equal to 1.1 at -10C and 1.0 for all temperatures above 0C (figure 3).

Spaans[9] adopted a simple equation also using the idler diameter ( $d$ ), but also includes a speed ( $v$ ) related component:

$$F_{id} = \frac{d}{0.133} \cdot (1 + 0.3 \cdot v)$$

In the CEMA 6<sup>th</sup> edition, the idler drag has been completely revised. It incorporates both speed and load into the new drag equation, as well as a temperature component. The temperature correction component ( $K_{IT}$ ) however is actually just the same  $K_t$  factor that was previously used in the 5<sup>th</sup> edition.

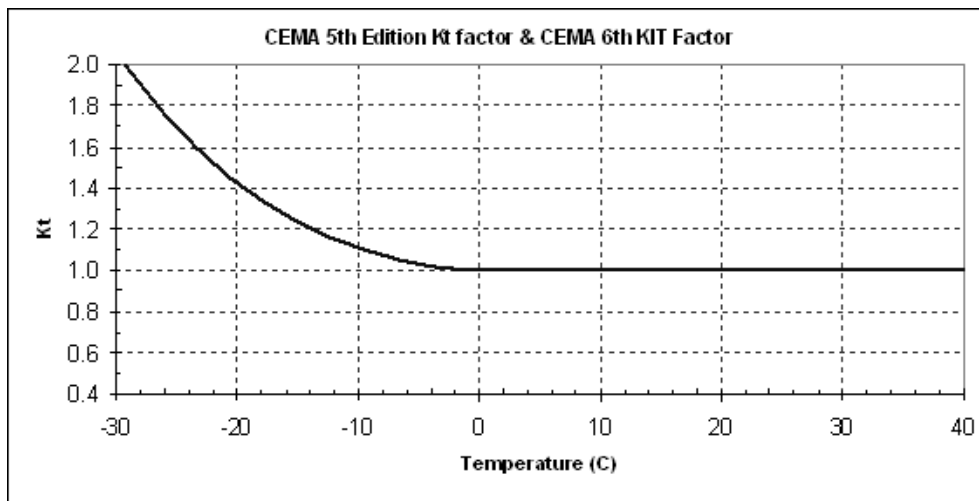


Figure 3 – CEMA 5<sup>th</sup>& 6<sup>th</sup> Editions use the same  $K_t$  Correction factors for Idler drag

Wheeler[10] separated the idler drag into two components; the bearing drag, and the manufactures seal drag. The drag values for sealed deep groove ball bearings generally do not vary significantly from manufacture to manufacture. The moment (and thus drag force) can be calculated by following the equations found in the SKF catalog [11]. This method divides the bearing drag into three components as follows:

$$M_t = M_{rr} + M_{sl} + M_{seal}$$

$M_{rr}$  = rolling frictional moment

$M_{sl}$  = sliding frictional moment

$M_{seal}$  = frictional moment from seals

The calculation of each of these items is a function of the bearing type, geometry, loading, speed, and grease viscosity. All of these items are known at design time, and thus implementing this methodology into a software program is relatively straight forward.

The manufacture seal drag however, can vary significantly from manufacture to manufacture (Figure 4). Most manufactures use a series of annual rings making up the labyrinth seal. Although the inner and outer diameters are the same for a given bearing, the total thickness, number of rings, and separating gap can vary significantly.

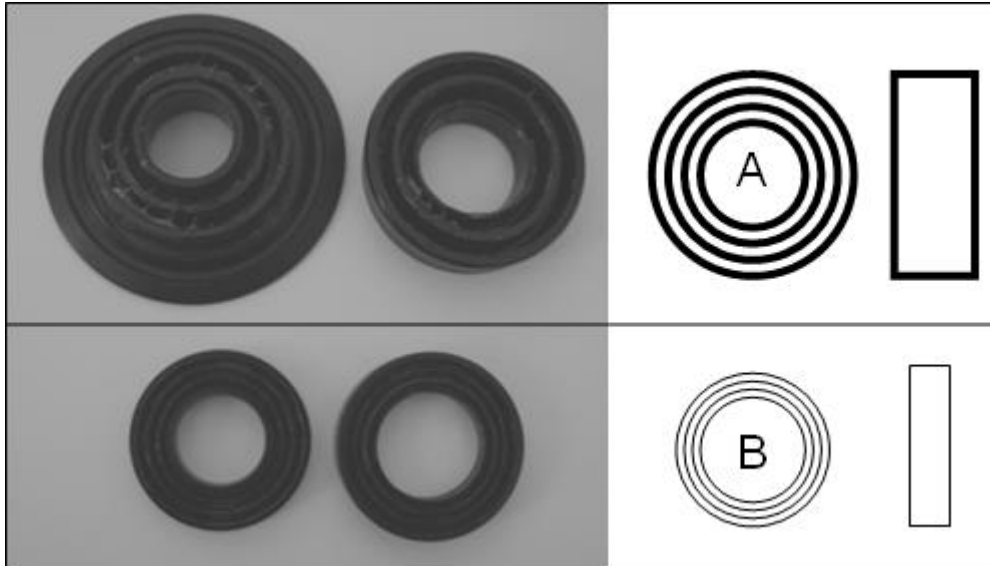


Figure 4 – End seal geometric differences between bearing types and manufacturers

The seal drag can be estimated by using the equation for viscous flow between parallel plates.

$$F_s = \frac{\mu \cdot V}{z \cdot l \cdot t}$$

Where:  $\mu$  = grease viscosity  
 $V_r$  = velocity at seal  
 $z$  = gap between seals  
 $l$  = circumference at seal  
 $t$  = thickness of seal

This calculation can be done for each ring of the labyrinth seals (usually 3 or 4). The outer rings have a higher velocity, and larger circumference, than the inner seals. This can easily be included in the calculations. Furthermore, most seals are only filled about 25%-40% with grease, and thus the seal force can be reduced to account for this. If the exact manufacture is unknown, average geometric values can be assumed for an estimated value.

It is interesting to note that this force is directly dependent on the grease viscosity, and inversely dependent on the seal gap. Furthermore, grease viscosity is strongly dependent on temperature. Grease viscosities are typically given at 40 C and 100 C. However, they follow a linear relationship on a logarithmic scale which allows easy extrapolation to most temperatures.

Figure 5 shows a typical test result of bearing drag measurements from Wheeler. Initially the drag force is approximately 6 N, but quickly drops to 4 N within 40 seconds. The drag stabilizes around 2.2 N, and the bearing temperature appears to be leveling off around 33 C. The initial torque is perhaps due to the grease setting inside the bearing and seal, and needing to be redistributed in the labyrinth.

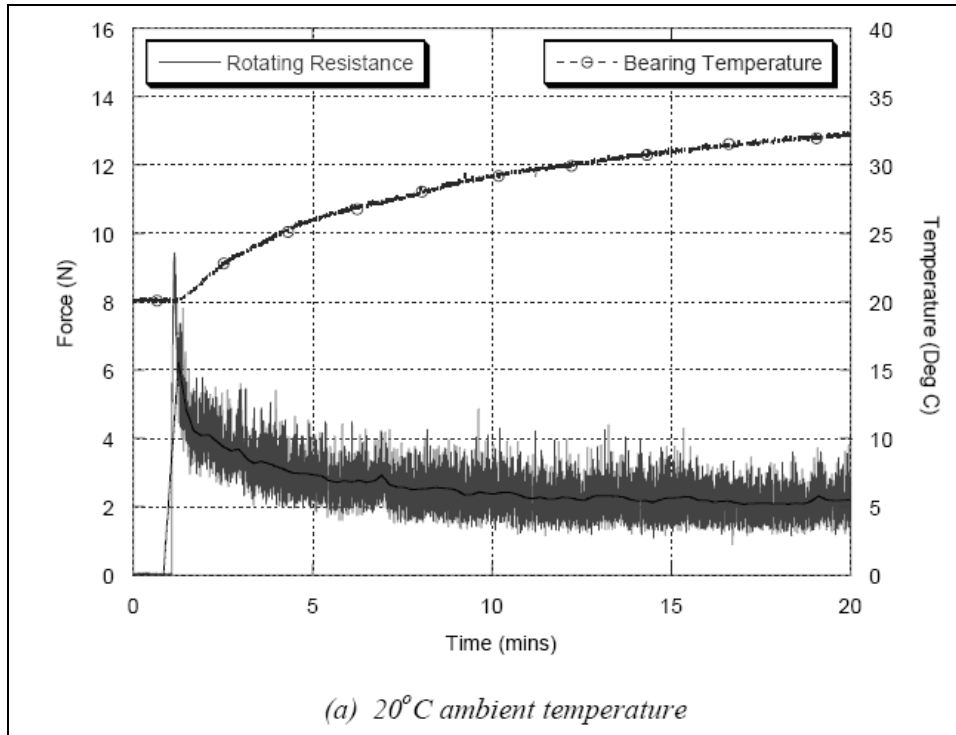


Figure 5 – Idler rolling resistance as a function of time

The question now becomes, for which point should the conveyor be designed? Conservatively one would choose 6 N. However, considering a 2 km conveyor may have over (5000 rolls), operating at 4.0 m/s, this would add approximately 76 kW of power over the steady state value of 2.2 N.

In the author's opinion, both values should be used. For steady state design purposes the stabilized idler drag should be used. This is also true for emergency stopping conditions. However, when analyzing the starting requirements for the conveyor, a higher drag value should be used. This can simply be a multiplier of the steady state value (say 1.5 – 3.0).

Figure 6 shows the idler drag per roll for 152 mm series 30 bearing using the calculation methods discussed above. For the theoretical method the bearing temperature was assumed to stabilize 15 degrees above the ambient temperature when calculating the grease viscosity.

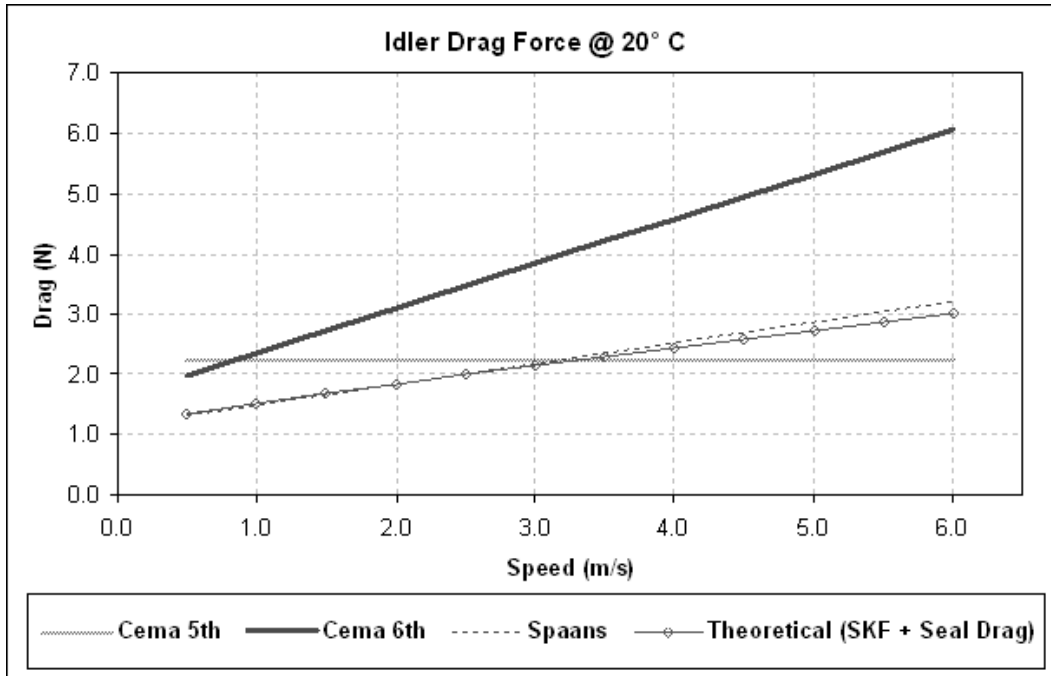


Figure 6 – Idler rolling resistance as a function of speed for various calculation methods

It is interesting to note that from the CEMA 5<sup>th</sup> edition, to the 6<sup>th</sup> edition the idler drag component has increased dramatically. At 5.0 m/s the 6<sup>th</sup> edition value is 5.3 N vs 2.2 N previously.

Figure 7 shows the drag values at a temperature of -10° C. The theoretical value has increase substantially due to the lower viscosity of the grease. However, the CEMA 6<sup>th</sup> values are still the highest.

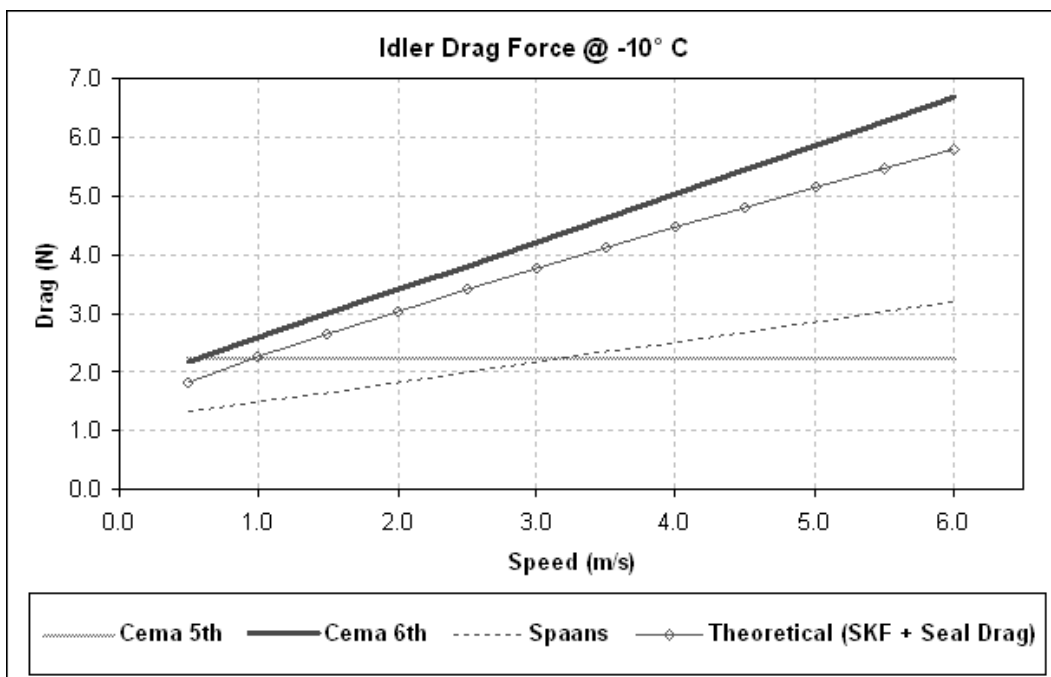


Figure 7 – Low Temperature Idler rolling resistance as a function of speed

There is no doubt that idler drag can vary significantly from manufacture to manufacture. For the most accurate calculations one should perform laboratory testing using the selected manufacture and specific operating environmental conditions (particularly for system

operating below 0° C). However, when this is not possible the author recommends following the theoretical approach described above.

The South African standard SABS 1313-1 states the idler drag at 20° C, and 650 RPM, for a 152 mm roll must not exceed 2.6 N. This is in line with the theoretical methodology (2.65 N). However, the new CEMA 6<sup>th</sup> method (5.2 N) is significantly higher the currently allowed value.

#### 4.2 IDLER ALIGNMENT

Because the idlers can not be perfectly aligned or constructed, misalignment forces must be taken into account. Although these forces can be theoretically calculated, a statistical deviation should be used to determine the true effects of these values.

In the CEMA 5<sup>th</sup> edition idler alignment was taken into account by the preceding “0.0068” factor used in the K<sub>x</sub> idler equation. This was simply:

$$F_{ia} = 0.0068 * W_{mb} * L$$

This equation make basic sense as it is a constant value per unit length. The skewing of an idler should result in the normal idler load being multiplied by a misalignment angle factor. Thus if the idler spacing is doubled, the corresponding load (and misalignment force) would also double, but for half as many idler sets. Therefore the net results would be the same.

In the CEMA 6<sup>th</sup> edition the idler installation has been subdivided into three parts:

1. Longitudinal misalignment (user selects alignment factor)
2. Inclination misalignment (for which the recommend value is zero)
3. Manufacturing tolerances (fixed value)

Item 2 represents a forward tilting of the idler set (which the default value is zero). The manufacturing tolerance is given as a single fixed value. To calculate the longitudinal misalignment the user must select one of four installation values (precise, none, imprecise, or unstable). Figure 8 shows the influence of the different methods for the CEMA 6<sup>th</sup> and 5<sup>th</sup> editions. This graph is for a 1600mm belt, running at 4.0 m/s, transporting material at 3000 T/H. Even with a precise installation tolerance the new CEMA 6<sup>th</sup> method give exceptionally higher drag forces. Furthermore, these values do not include any inclination (forward tilt) drag forces as the author has used the zero default value.

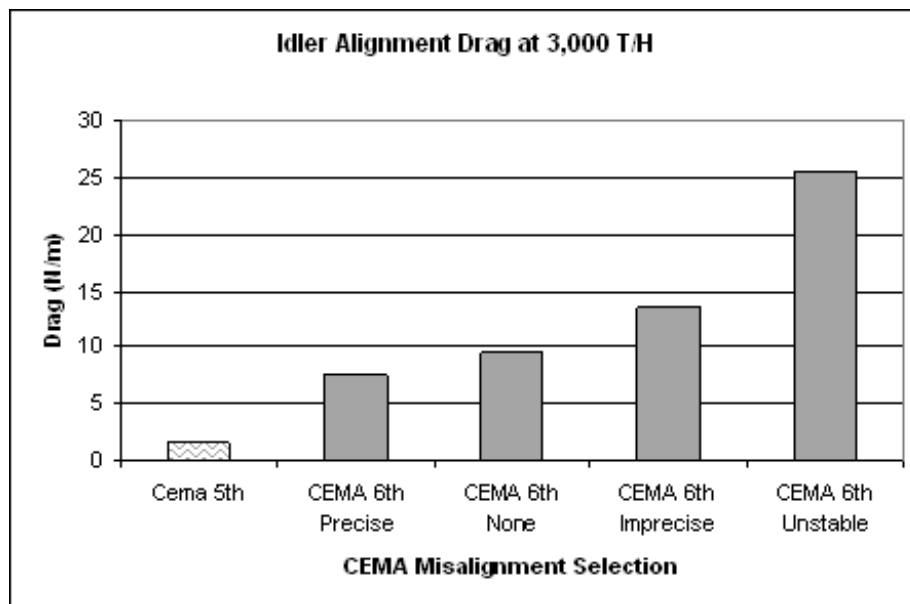


Figure 8 – Idler Misalignment Effects – CEMA 5<sup>th</sup> and 6<sup>th</sup> Editions

## 5. BELT LOSSES

### 5.1 ROLLING INDENTATION

As the belt passes over the idler, its bottom cover rubber is slightly compressed resulting in a negative drag component. As the belt leaves the idler, the rubber is uncompressed resulting in a positive force. If the rubber were a perfectly elastic material, these compression and restoring forces would balance and the net drag would be zero. However, real rubber compounds are not perfectly elastic, and thus an overall drag force results. Quantifying this drag force has been the subject of countless papers by a variety of authors.

In 1959 May et al [12] published a paper entitled "Rolling Friction of a Hard Cylinder over a Viscoelastic Material". This paper laid the ground work for future development in this area. In 1980 Jonkers [13] published a method for calculating this effect on a troughed belt conveyor. Jonkers method incorporated the belt's viscoelastic properties as well as the belt speed, idler diameter, and vertical loading. Since then numerous papers have been published with variations and additions to this basic theory. Wheeler[10] compares some of these methods to a finite element model and experimental measurements he obtained. Figure 9 shows an example of his results:

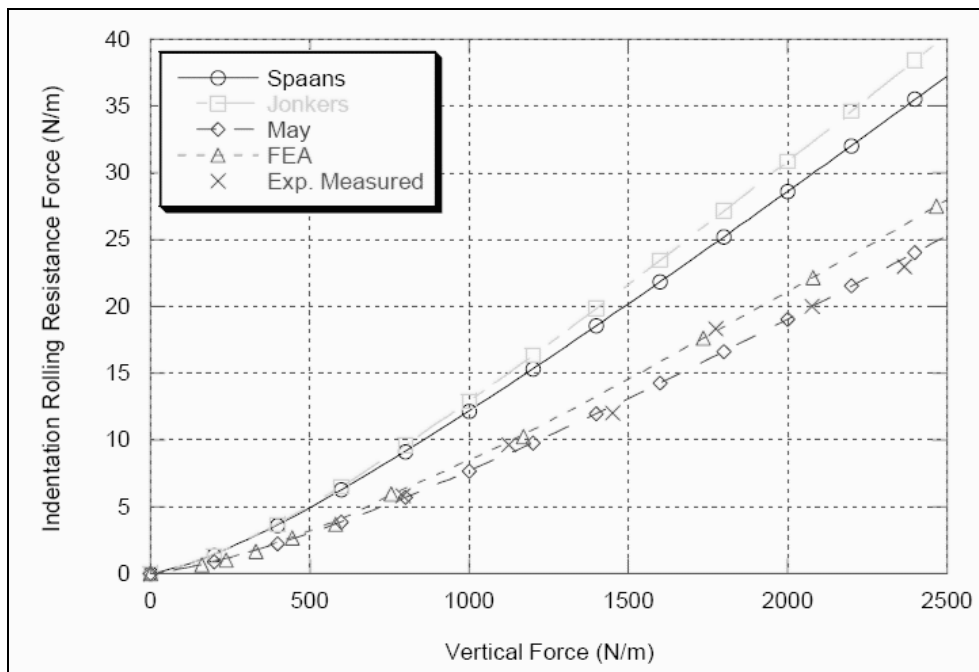


Figure 9 – Indentation Rolling Resistance Losses vs Vertical Loading (Wheeler)

However, in order to use any of these calculation methods the belts cover rubber properties must be obtained. These properties are typically a function of both frequency and temperature, and often determined using time-temperature superposition to generate a "Rheological Master Curve". This requires a rubber rheology test machine similar to that shown in figure 10. This however, opens up yet another hotly debated subject regarding the proper testing procedure, sample geometry, and so on. For the reader's sanity, the author will skip these details and simply reference the supporting literature. [4, 8, 10, 15].



Figure 10 –Rubber rheology instrument used to determine belt cover properties

The CEMA 5<sup>th</sup> edition combines the rolling resistance and belt/material flexure all into a single equation which was empirically derived. Due to this combination these methods cannot be directly compared.

The CEMA 6<sup>th</sup> edition does include a rolling indentation calculation methodology. The equations, and material properties for a specific belting compound, are given in chapter 6 of the CEMA book. Figure 11 shows a comparison between CEMA, Jonkers, Greune & Hager [15], and Oszter, Behrends, and Vincent (OBV method) [16]. With the exception of the OBV method, loss factors are given for both fabric and steel cord belting.

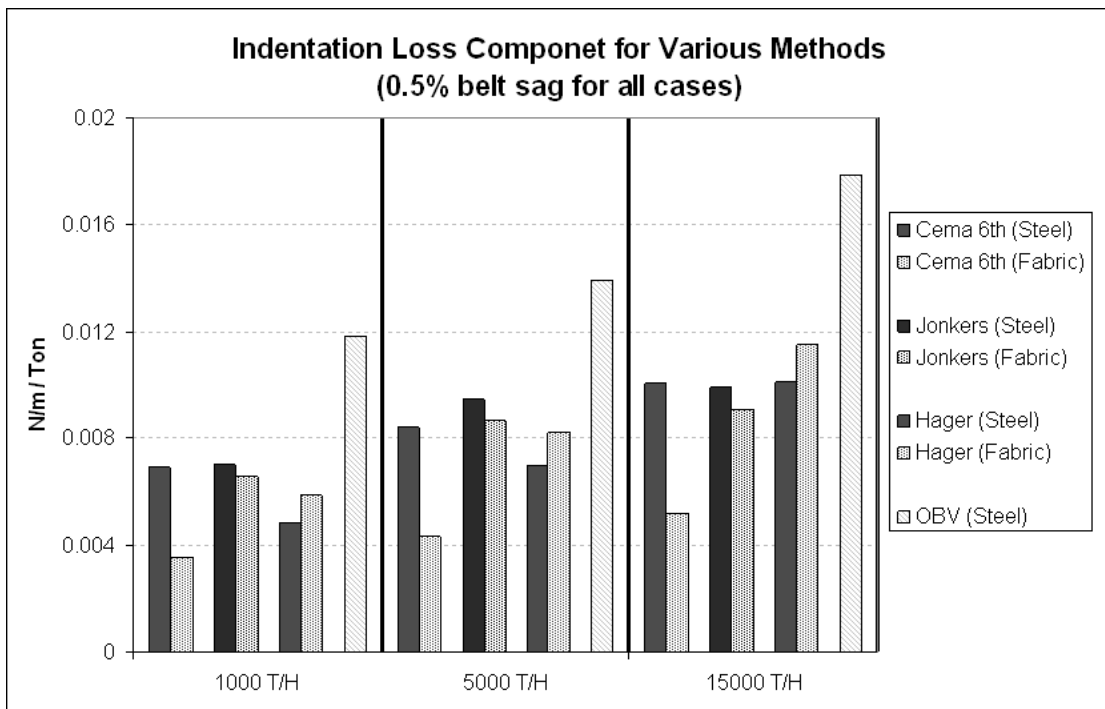


Figure 11 – Indentation loss component for various methods and steel cord vs. fabric belts

One of the constants used in the CEMA 6<sup>th</sup> equations ( $b_0$ ) is multiplied by the overall indentation value. This value is set to 0.14 for steel cord belts, and 0.072 for fabric belting. Therefore the indentation losses for a steel cord belt will *always* be twice as much as that of an equivalent fabric belt (assuming the same rating, tensions, cover thickness, etc).

Jonkers predicts a slight decrease in power consumption for steel cord belts due to the higher belt modulus. However this reduction is less than 10%. Greune and Hagar make a direct comparison of steel cord vs fabric belting, and also provides experimental measurements (Figure 12). Their data shows a small increase in the loss component with fabric belting. They attribute this to the stiffer backing of the fabric and increased flexing losses in the fabric layers.

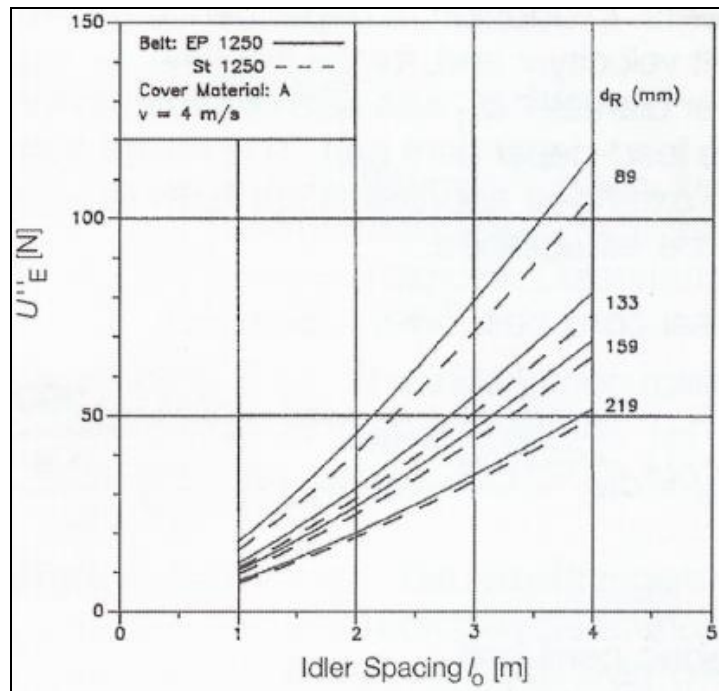


Figure 12 – Indentation loss comparison for fabric and steel cord belts

The OBV method does include a factor of 0.85 for steel cord belting. However, the paper doesn't explicitly state that fabric belting should use a factor of 1 (or some other value). Therefore only the steel cord value was shown in figure 11. Although the OBV is significantly higher than the others, it should be noted that this methodology was developed specifically for high tonnage applications (>12,000 TPH), and obtained from actual field measurements.

## 5.2 BELT FLEXURE

Due to the flexibility of the belt, it sags and flattens (opens up) between the idler sets. This flexing results in a hysteresis loss which can be quantified. Spaans[9] developed an explicit equation for this item as does the OBV method[16].

The CEMA 6<sup>th</sup> edition combines both the belt flexure and material trampling into a single equation and thus comparative results between these methods will be performed in the next section.

AC-Tek has developed a full 3D model using finite element analysis (FEA) in order to determine the actual belt shape and flexural losses (Figure 13). This model incorporates the belts non-linear structure and requires a number of advanced FEA components (stress stiffening, non-linear analysis, large displacement theory, contact elements, etc). Now that this parametric model has been constructed it is routinely used for analyzing belt flexure, idler junction stresses, fatigue properties, and many other belting design obstacles facing the industry today.

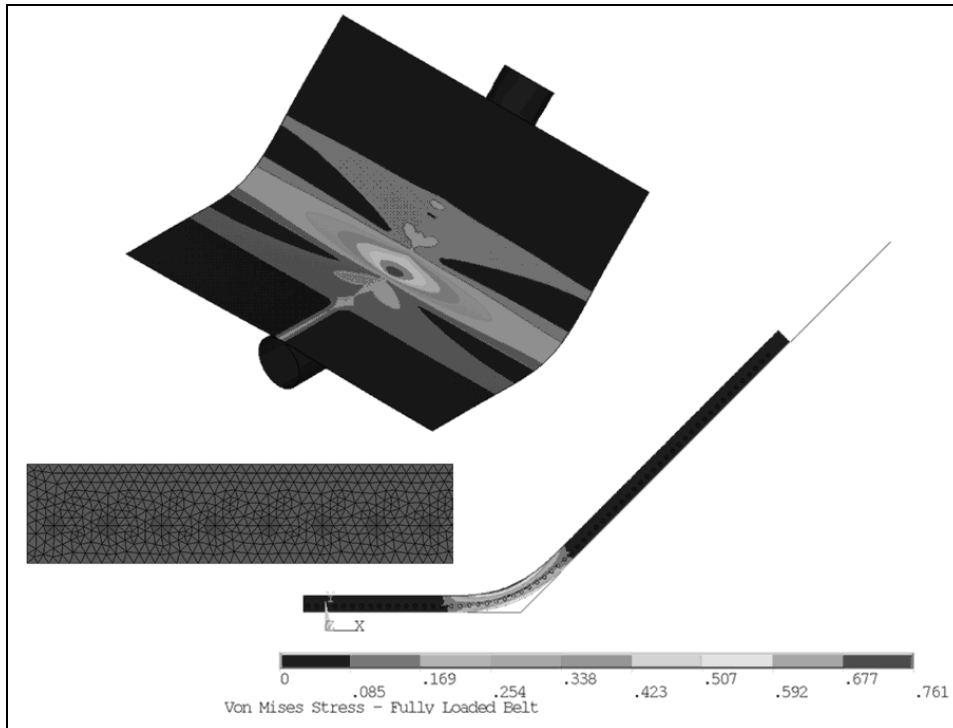


Figure 13 – Finite element belt flexure and deformation model

### 5.3 MATERIAL TRAMPLING

In addition to belts flexural loss, material trampling must also be taken into account. In the vertical plane material is lower and lifted as it travels between idlers sets. Transversely the troughed belt flattens out between idlers allowing the material to expand. It is then forced back to its original shape as it passes through each idler set. Throughout this process the material experiences internal shearing forces, alternating between active and passive states. This “trampling” loss component can be significant and is perhaps one of the most difficult of all components to accurately determine. This is primarily due to the fact that its value can not be directly measured in a controlled laboratory test. Instead the total losses for a system are measured, and then each of the *known* individual parts is subtracted. What remains is considered to be the trampling component. Harris[17], presented some preliminary measurements. Spaans developed a closed form equations for material flexure, however he also noted that his model should only be used for qualitative consideration. Furthermore it was dependent on the belts minimum curvature over the idlers for which no direct equation was derived. The OBV method presents a closed form solution for a 3 roll 35 degree and 45 degree set. However his formula assumes the belt was full loaded and operating at 1% belt sag. He combined both belt flexure and trampling into the following equations:

$$T_{bf} + T_{mf} = 0.75 * W_{mb}^{2.26} / T_{avg}^{0.83} \text{ (35 degrees)}$$

$$T_{bf} + T_{mf} = 1.28 * W_{mb}^{2.06} / T_{avg}^{0.76} \text{ (45 degrees)}$$

As with rolling resistance, the 5<sup>th</sup> edition of the CEMA equations does not discern between belt flexure, material flexure, and indentation losses (all lumped into the  $K_y$  value).

The 6<sup>th</sup> edition CEMA equations have included a method to calculate the combined belt flexure and trampling components. Figure 14 shows the trampling loss for a conveyor running at 4 m/s. The sag was set at 0.5% and 1.5% for tonnages of 1,000 T/H (Coal – 1200mm belt), 5,000 T/H (Copper – 1200mm belt), and 15,000 T/H (Copper – 2000mm belt).

CEMA 6<sup>th</sup> predicts that the loss in a fabric belt will be approximately 3 to 5.5 times higher than a steel cord belt. No explanation is given for this significant difference.

The differences in results between the fabric and steel cord belt construction for the CEMA method are considerable. While it is true that a fabric belts can have almost double the flexural loss of a steel cord belt due to its construction. It is also true that the belt flexural component is typically much less (10%-20%) than the material flexural component. Additionally, at 0.5% belt sag, the deformed shapes of a steel cord belt and fabric belt are quite similar. As the material trampling loss is only a function of this deformed shape, one would expect the losses to also be similar.

The OBV equations follow an increasing pattern. At 0.5% sag, the N/m/ton value increase as would be expected. The same is true at 1.0% sag, and from 0.5 to 1.0% at each tonnage. No such pattern exists for the CEMA 6<sup>th</sup> data where the maximum loss occurs at 5000 T/H and not 15000 TPH as would be expected.

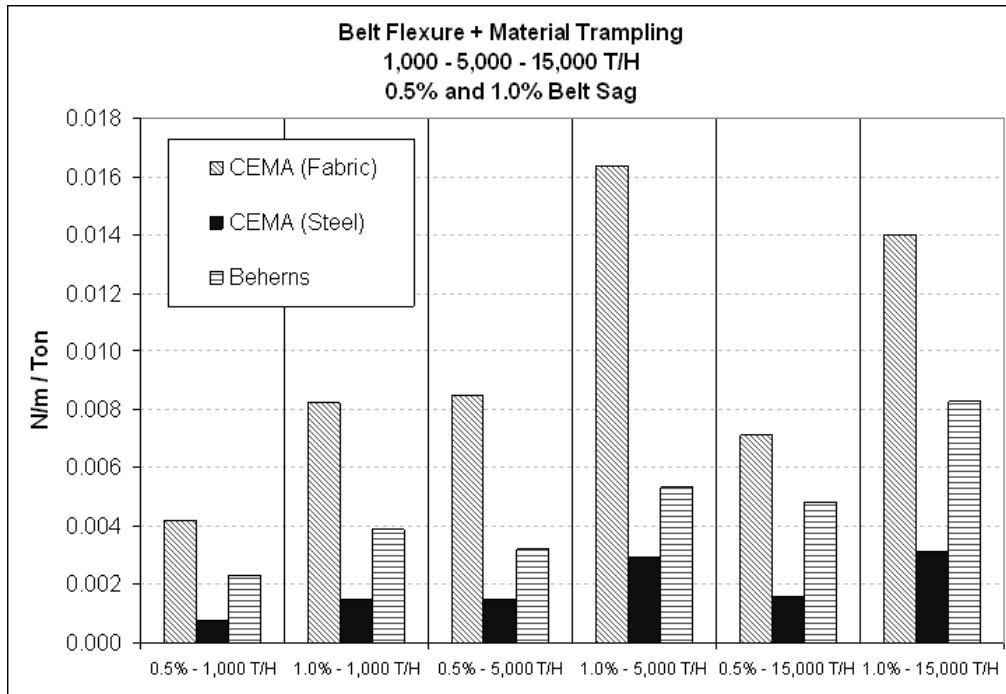


Figure 14 – Belt Flexure & Material Trampling Loss Components

Due to the complex nature of this problem, computer modeling offers significant insight into this problem. By combining the belt flexure FEA model discussed above, with discrete element analysis (DEM), a quantitative model can be developed. Figure 15 shows a DEM/FEA simulation. The FEA provides the geometry, while the DEM simulation gives results for the loading forces, and internal material losses.

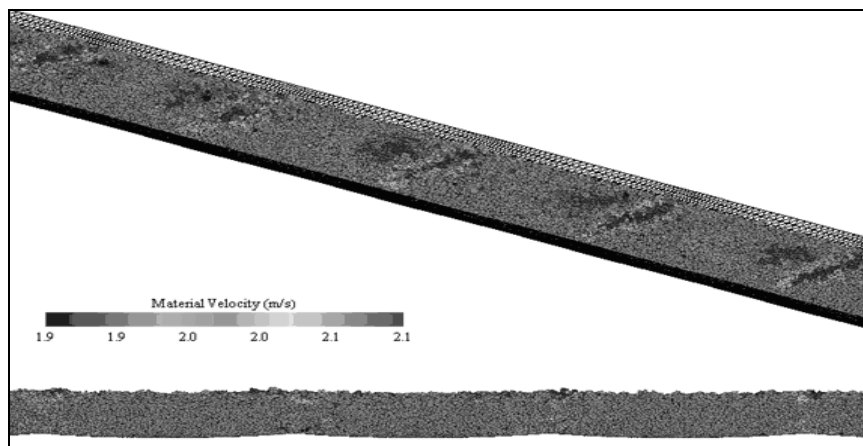


Figure 15 – Combined FEA/DEM simulation for material trampling losses

## 6. MECHANICAL LOSSES

### 6.1 REDUCER LOSSES

Reducer losses are typically on the order of 1.5% per stage. Thus a 3 stage gearbox would have around 4.5% losses. These losses are primarily due to the churning of the oil. However, what reducer manufacturers fail to emphasize is that these losses are only representative when the reducer is operating at 100% power. At lower power values the losses (as a percentage of the transmitted power) are significantly higher. Migliore [17] did extensive research and testing in this area. It was shown that the losses could be calculated as follows:

$$T_{gb} = (P_o + (1 - P_o) * T_o) * (1 - \text{eff} / 100) * T_{np}$$

Where:

$P_o$  = Constant value which is a function of the reducer

$T_o$  = Torque at operating condition

Eff = Reducer Efficiency at 100% power

$T_{np}$  = Tension developed at 100% rating

### 6.2 FLUID COUPLINGS

If fluid couplings are used on the system these losses need to be taken into consideration as well. Fluid couplings will generally result in 4%-8% power loss depending on the specific coupling and various other factors (fill levels, oil viscosity, transmitted power, etc).

### 6.3 PULLEY BEARING LOSSES

Pulley bearing losses can be easily estimated. The CEMA 5<sup>th</sup> edition simply used a constant value of 900N (200lbs) for driven pulleys and 670N (150 lbs) for non-driven pulleys. The 6<sup>th</sup> edition of CEMA has copied the ISO 5048 equations which subdivides the loss into two components. The first component accounts for the loss due to the belt flexure over the pulley. Separate equations are given for fabric and steel cord belts. Unfortunately however, these equations do not take into account the wrap of the belt around the pulley as one would logically expect. However, if it is assumed that the equations are given for 180 degrees of wrap, the result can simply be scaled for the actual wrap angle.

$$T_{\text{fabric}} = 9 * B_w * (140 + 0.01 * F / B_w) * d / D * c$$

$$T_{\text{steel}} = 12 * B_w * (200 + 0.01 * F / B_w) * d / D * c$$

Where:  $c$  = actual wrap angle / 180

$F$  = Normal Force on Pulley (N)

$B_w$  = Belt Width (mm)

$d$  = Shaft Diameter (mm)

$D$  = Pulley Diameter (mm)

The second part of loss calculation is dependent on the total normal load on the pulley. It is given by:

$$T = 0.1 * d * F / D$$

Unfortunately, neither of these equations include the pulley RPM. As shown in the idler drag calculations discussed previously, the speed can have a significant effect on bearing drag and thus should be included. In the author's opinion, if one is going through the effort to include pulley drag losses, then the standard SKF calculations are the best choice. They are slightly more complex, but can still easily be added to any computer program or spreadsheet calculation [18].

### 6.4 MINOR LOSSES

The list of minor belt losses is extensive, but includes belt cleaners, discharge plows, and skirtboard losses to mention a few. Losses for these components can vary widely from

different manufactures, as well as from actual installation settings. One should not however overlook these items, particularly on small conveyors.

## 7. THEORETICAL COMPARISONS

### 7.1 COMBINED IDLER & BELT LOSSES

This section will compare the combined results of sections 4 and 5. This is useful as it allows a more direct overall comparison to be made between methods, while still excluding material lift, mechanical losses, and other minor losses.

The bar graphs in figures 16-19 show the tensions calculations at a single point (element) on the carry side of the conveyor. The conveyor parameters for each case are:

- Case 1: 1,000 T/H - 1200mm belt - 4.0 m/s – Coal – 1.5m Si – 1.0% Sag
- Case 2: 5,000 T/H - 1200mm belt - 4.0 m/s – Copper – 1.5m Si – 1.0% Sag
- Case 3: 15,000 T/H - 2000mm belt - 4.0 m/s – Copper – 1.0m Si – 1.0% Sag
- Case 4: 15,000 T/H - 2000mm belt - 4.0 m/s – Copper – 1.0m Si – 0.5% Sag

For the DIN/ISO method the equivalent friction factor was simply set to 0.020 for all cases. In general this value is typically lower than 0.020 for lower tonnage conveyors, and higher for higher tonnage conveyors. The idler alignment was set to “precise angular alignment” for all CEMA 6<sup>th</sup> calculations. The “JSB” method uses the Jonkers equation for idler indentation, Spaans idler drag, the OBV method for material and belt trampling, and the CEMA 5<sup>th</sup> method for idler misalignment.

All values are given in N/mm so that a 1 to 1 comparison can be made. Furthermore, the conveyor power is simply the tension differential times the belt speed, and thus the relationships in these graphs would be the same if converted to demand power.

It is very important to remember that these comparisons are completely independent of the conveyor length. The calculations are performed at a specific belt sag and tension value.

At 1,000 T/H, case 1 represents light tonnage conveyors. In this case the CEMA 5<sup>th</sup> methodology results in the highest N/mm tension value, while the JSB method is the lowest. It would not be uncommon however for an engineer to choose a DIN/ISO value of 0.016 for lower tonnage conveyors. In this case the DIN/ISO and the JSB model would match up fairly well.

At 5,000 T/H case 2 shows a very good comparison across the board for all methods except the CEMA 6<sup>th</sup> fabric belt. For this case the material flexure component is significantly higher than all other cases. The resulting N/mm tension is approximately double the other calculation methods.

At 15,000 T/H, case 3 the situation is reversed. CEMA 6<sup>th</sup> methodology has very low material trampling losses, which is surprising due to the high material tonnage. This method, with a fabric belt, results in very low tension loss values. CEMA 5<sup>th</sup> and Jonkers models match quite well. Also, it would not be uncommon for a designer to use a DIN/ISO value of  $f=0.030$  for a high tonnage conveyors like this. This would increase its value to 375 N/mm and thus match up very well with the CEMA 5<sup>th</sup> and the JSB methods.

Case 4 is identical to 3 except the belt tension was increased to give 0.5% sag. Again the CEMA 6<sup>th</sup> fabric belt gives the lowest losses.

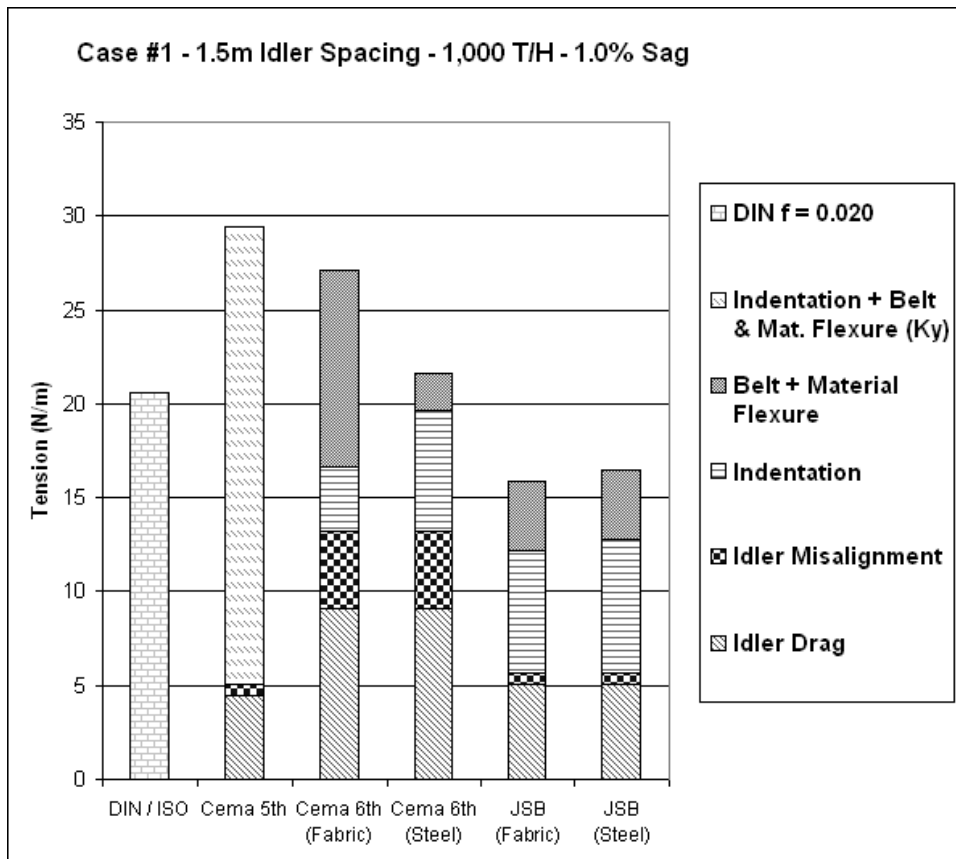


Figure 16 – Tension Components at 1.0% Sag and 1,000 T/H

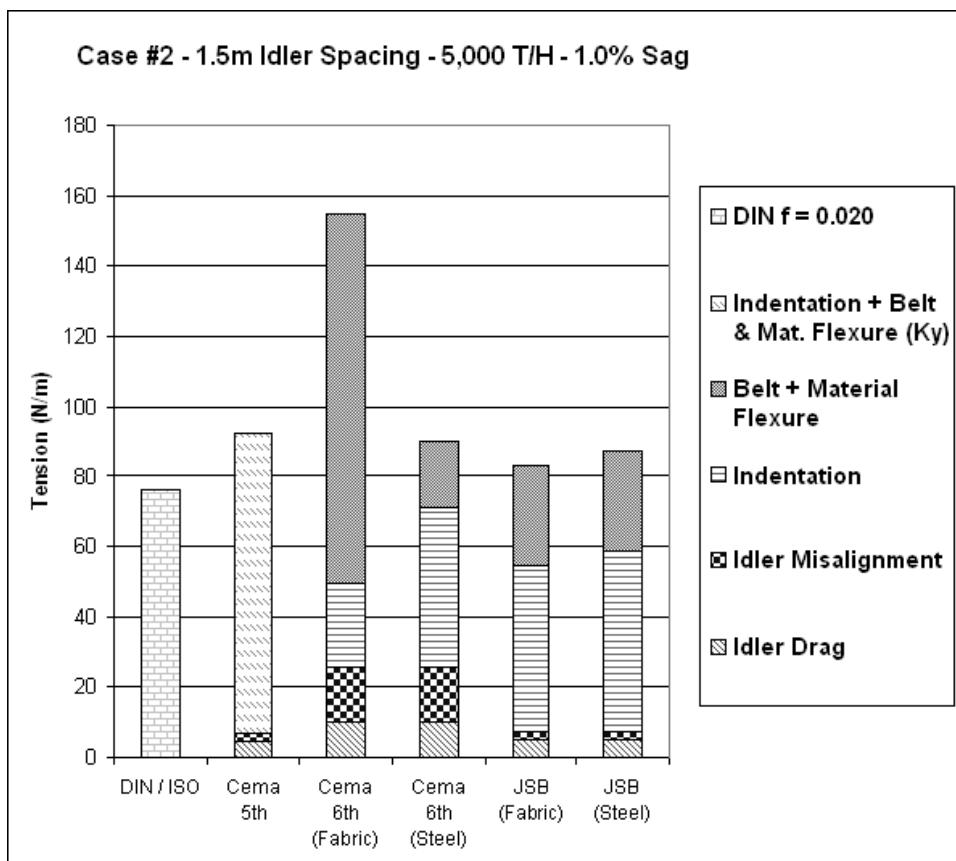


Figure 17 – Tension Components at 1.0% Sag and 5,000 T/H

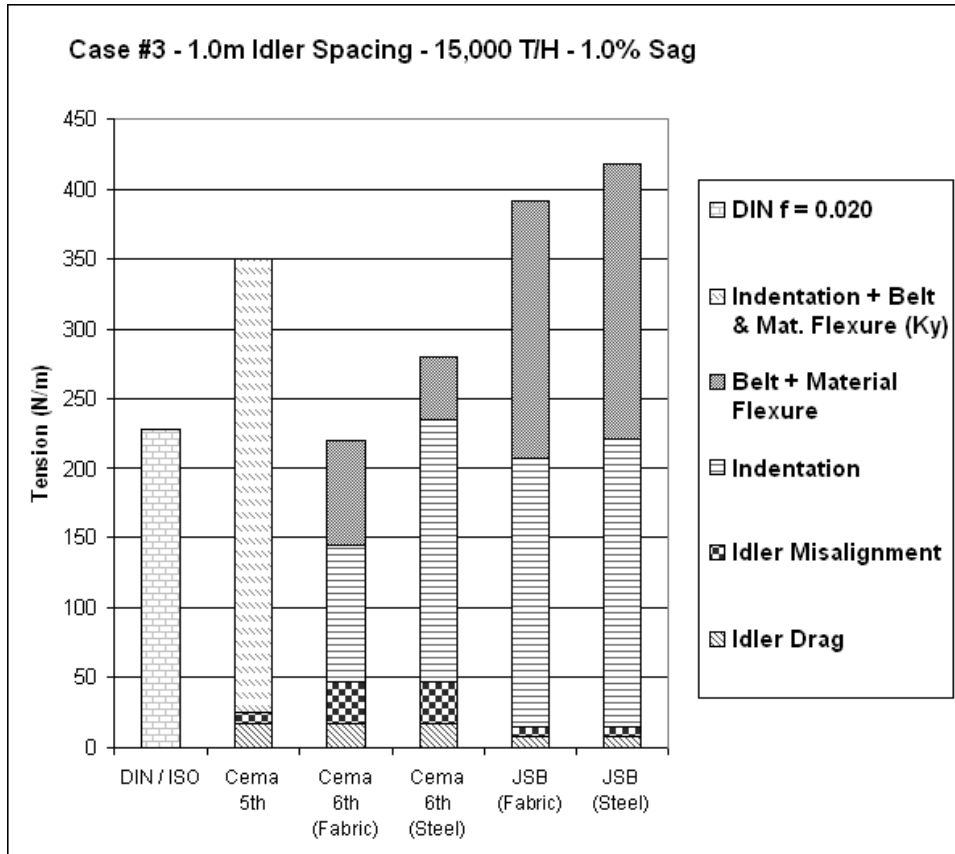


Figure 18 – Tension Components at 1.0% Sag and 15,000 T/H

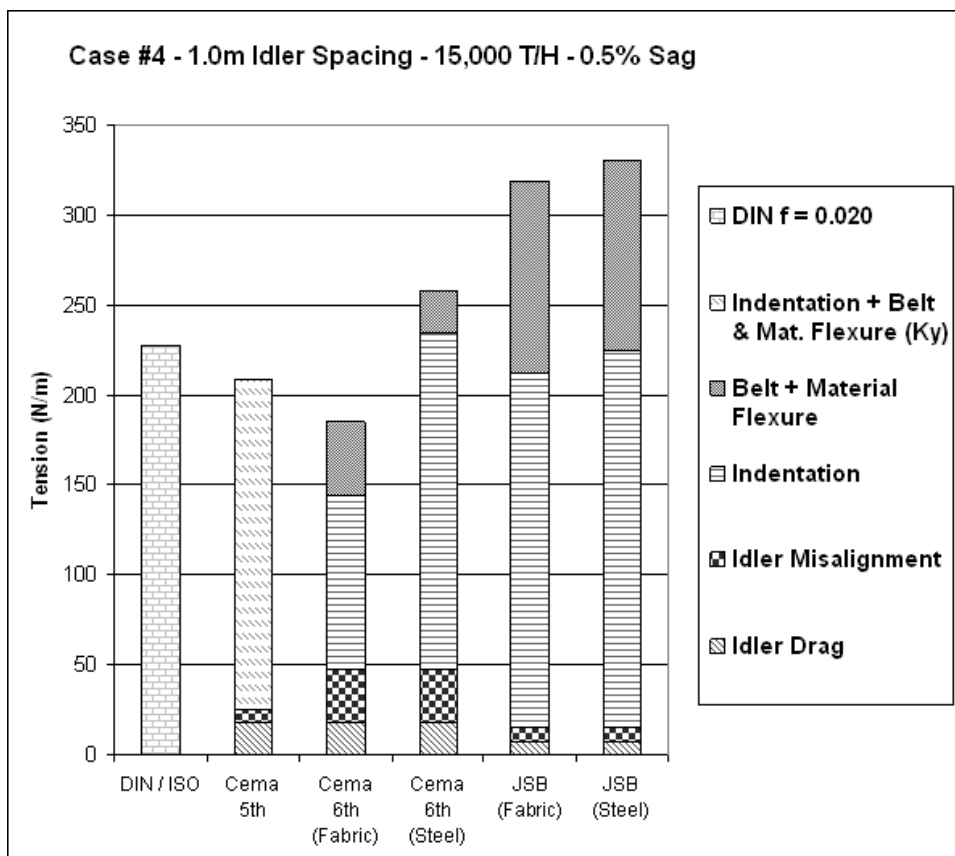


Figure 19 – Tension Components at 0.5% Sag and 15,000 T/H

## 7.2 OVERLAND CONVEYOR FIELD MEASUREMENTS

It is only prudent to now compare the previously discussed calculation methods with some real world conveyor measurements. Acquiring accurate field measurements is not a trivial exercise. The authors have taken detailed field measurements on a wide range of conveyor system around the world [5, 6, 7]. For this paper three specific installations will be investigated. The three conveyors represent low, medium, and high tonnage applications. Additionally, the data on these conveyors is readily available in the public domain from a variety of sources. The case studies to be investigated are:

1. Sasol Wonderwater Conveyor S06 (2,000 T/H)
2. Muja Collie (750 T/H)
3. Goodyear case study conveyor (10,000 T/H)

The demand power for each conveyor is estimated with the DIN 22101, Cema 5<sup>th</sup>, CEMA 6<sup>th</sup>, and the combined “JSB” method described in section 7.1. The DIN method assumes an equivalent friction factor of 0.020 for all three conveyors.

Each conveyor is analyzed and then compared to the actual published field measurement. The demand power is graphed in the same fashion as section 7.1 (showing the breakdown of the individual components). Finally, the lift component of the total demand power has been removed from both the field measurement and calculated demand powers. This was done so that the individual components for the different methods are easier to compare.

The Sasol Wonderwater conveyor S06 is detailed by Pretorius[20]. This conveyor is located in South Africa. This conveyor is 3320 m long and has a design tonnage of 2000 T/H. The belt speed is 4.6 m/s. The conveyor is generally flat but has an overall elevation drop of 5.5 m. Figure 20 shows the results of the calculated demand powers. All four methods are higher than the published measurement. The JSB method is closest and is 6% high. CEMA 6<sup>th</sup> has the largest error and is 32% high.

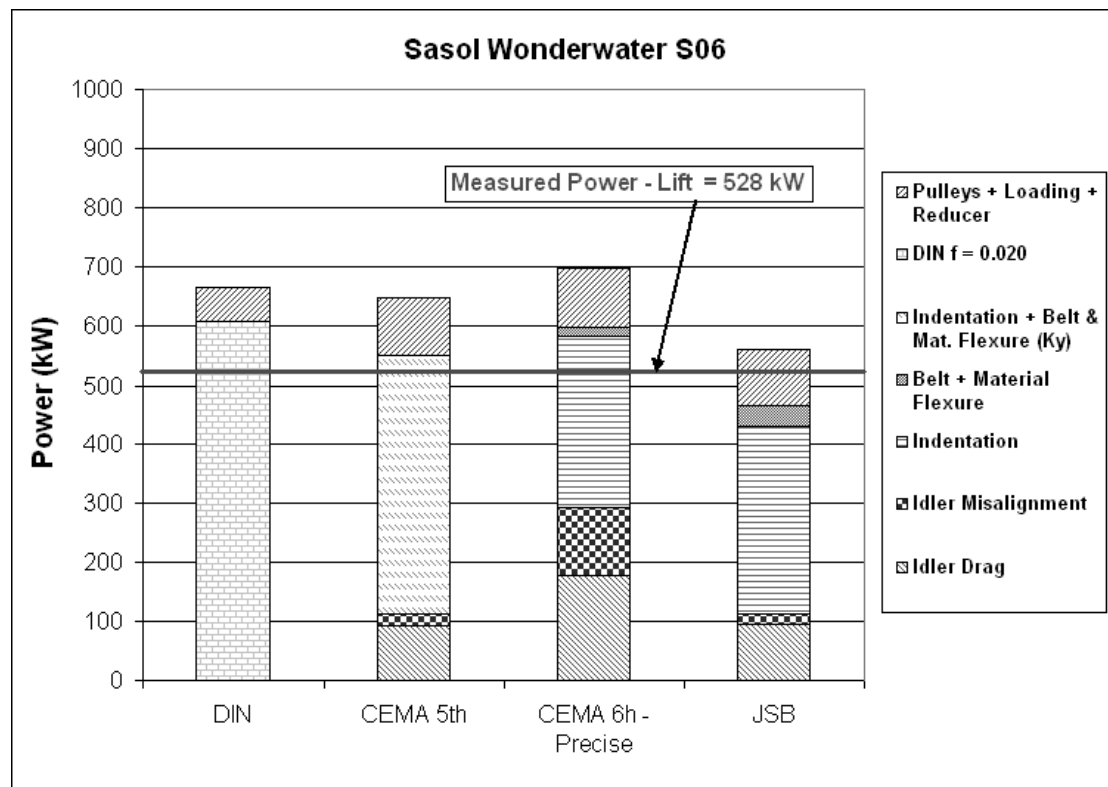


Figure 20 - Sasol Wonderwater Conveyor S06 – Field data vs various calculation methods

The Muja Collie conveyor [7] is located in Australia. This conveyor is 6110 m long and has a design tonnage of 770 T/H. The belt speed is 4.4 m/s. The conveyor is generally flat but has an overall elevation rise of 14.5 m. The field measurement was completed at 750 T/H, and so the demand power calculations are done at the same. Figure 21 shows the results of the calculated demand powers. Again, all four methods are higher than the published measurement. The JSB method is closest and is 43% high. CEMA 6<sup>th</sup> has the largest error and is 106% high.

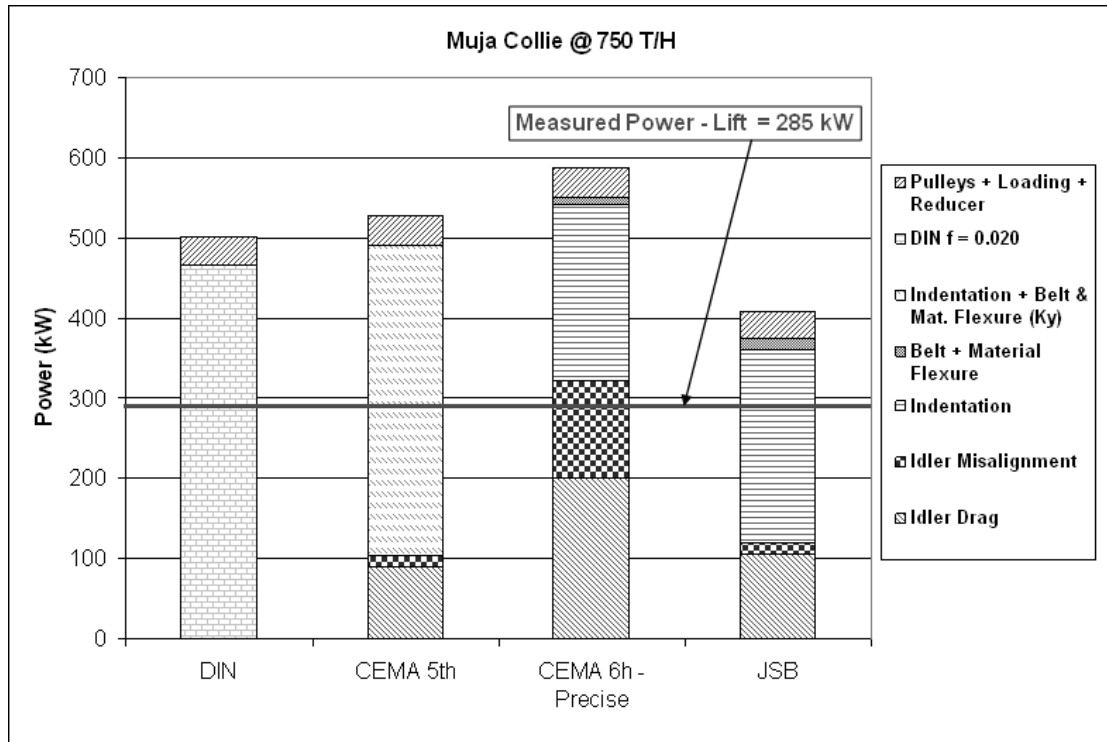


Figure 21 - Muja Collie Overland Conveyor – Field data vs various calculation methods

The last conveyor is detail by Gallagher [21]. The conveyor transports copper ore with a design tonnage of 10,000 TPH.

This conveyor is 2075 m long and has an overall elevation rise of 66 m. Two separate measurements were taken on this conveyor. The belt on this conveyor was replaced with a low rolling resistant belt. The first set of measurements, labeled Compound A, was completed before replacement of the belt. Then soon after installation of the low rolling resistant belt (Compound B) the second set of measurements were taken. Gallagher reports that demand power dropped by 310 kW with the low rolling resistant belt.

Figure 22 shows the results of the calculated demand powers. The JSB and DIN methods approximate Compound B (low rolling resistant) belt fairly well whereas the two CEMA methods are low. CEMA 6<sup>th</sup> is 8% lower than Compound B. However, all the methods are lower than the original belt (Compound A). The worst case, CEMA 6<sup>th</sup>, is 23% low.

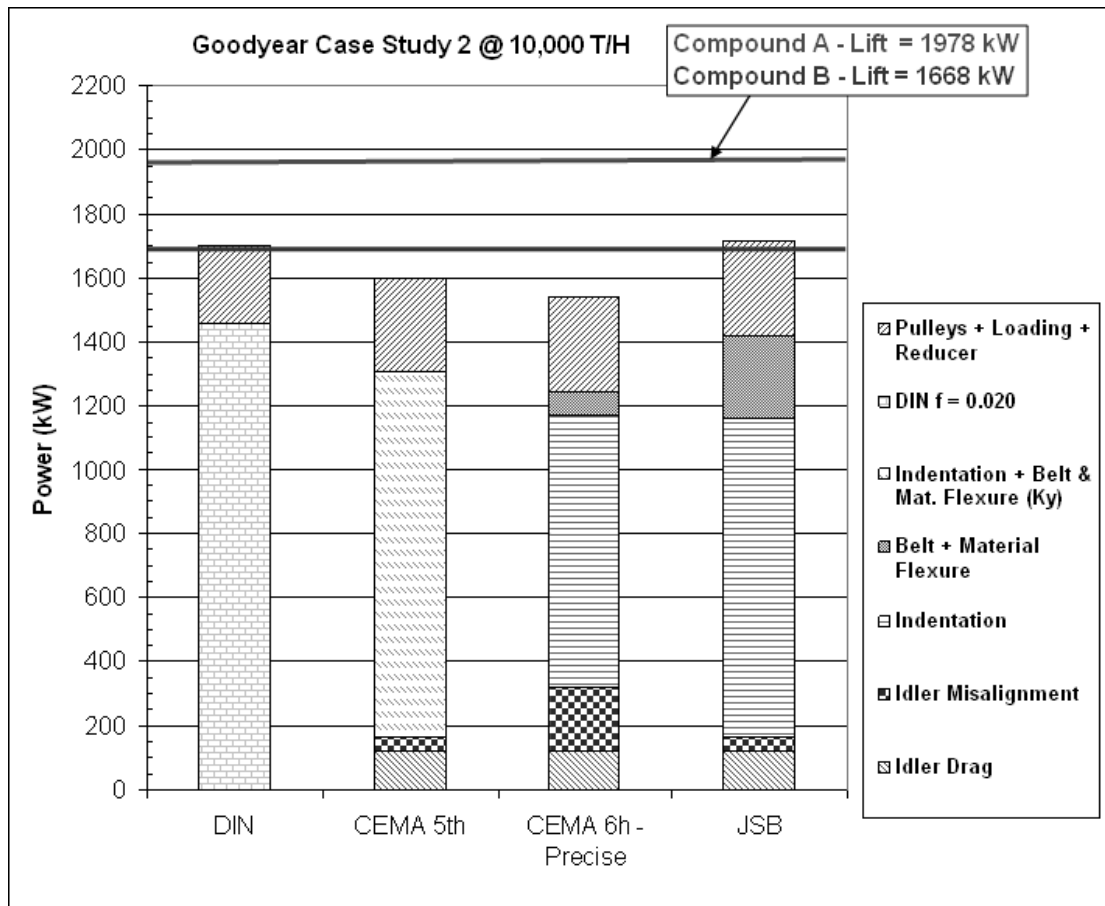


Figure 22 - Goodyear Case Study 2 – Field data vs various calculation methods

These three examples compare real life measurements to published calculation methodologies. At low tonnages, it seems that the methods overestimate the demand power. However, at high tonnages the methods underestimate the demand power.

## 8. CONCLUSION

This paper has described various calculation methods in use today. Individual tension components have been discussed in detail and compared to published data. A direct comparison was made between these methods and three real world conveyor systems.

After investigating and comparing existing methods, it is clear that there is still plenty of research yet to be done. This is particularly true for both long overland conveyors and high tonnage systems. Furthermore, in-house proprietary calculations methods are recommended if an optimized conveyor design is to be achieved in the most economical manner possible.

## REFERENCES

- [1] International Standard ISO 5048-1989 (E): Continuous mechanical handling equipment – Belt conveyors with carrying idlers – Calculation of operating power and tensile forces; Second edition 1989-09-15
- [2] DIN 22101: Belt conveyor for bulk materials – Bases for calculation and design; German Standards Organization; February 1982
- [3] CEMA “Belt Conveyors for Bulk Material – 5<sup>th</sup> Edition” Conveyor Equipment Manufacturers Association, 1997
- [4] CEMA “Belt Conveyors for Bulk Material – 6<sup>th</sup> Edition” Conveyor Equipment Manufacturers Association, 2005
- [5] Kruse, D. J. “Data Acquisition Techniques and Measurement Equipment for Belt Conveyors”, BELTCON 13, 2005
- [6] Kruse, D. J. “State-of-the-Art Data Acquisition Equipment and Field Measurement Techniques for Conveyor Belts”, SME Annual Convention, 2004
- [7] G. Lodewijks & D. Kruse “The Power of Field Measurements - Part I”, Bulk Solids Handling, issue 3/98, pg. 415-426, 1998
- [8] Lodewijks, G. “Determination of rolling resistance of belt conveyors using rubber data: fact or fiction?”, BELTCON 12, 2003
- [9] Spaans, C: The calculation of the main resistance of belt conveyors; bulk solids handling, Vol 11 (1991) No 4, pp 809-826.
- [10] Wheeler, C. - Thesis, Newcastle University, Australia
- [11] SKF, General Catalog, June 2003, pp 87-96.
- [12] May, W., Morris, E. and Attack, D.: Rolling Friction of a Hard Cylinder over a Viscoelastic Material; Journal of Applied Physics Vol. 30 (1959) No.11, pp.1713-1724
- [13] Jonkers, C.O.: The indentation rolling resistance of belt conveyors – A theoretical approach; Fordern und Heben Vol 30 (1980) No. 4, pp. 312-317
- [14] Nordell, L. “The Channar 20 km Overland”, Bulk Solids Handling, Vol 22, No4, Nov 1991 pp 275- 284
- [15] Greune A, Hager, M.: The Energy-Saving Design of Belt Conveyors; Bulk Solids Handling Vol. 10 (1990) No.3 pp. 41-45.
- [16] Oszter, Z.F., Behrends, W.K. and Vincent, D: Large capacity belt conveyor – motion resistance evaluation; Technical Papers, Mining Engineering, December 1980, pp 1715-1721
- [17] Harris, A “Measurement of Belt-Idler Interactions and Material Flexure Coefficient for Design of Troughed Conveyor Systems”, Bulk Solids Handling, Vol 7, No 3, June 1987, pp 83 - 87
- [18] Migliore, P “Laboratory Testing of Drivetrain Component Efficiencies for Constant-Speed and Variable-Speed Wind Turbines”, Global Energy Concepts, Nov. 4 1997
- [19] Sidewinder Conveyor Design Software Program, Advanced Conveyor Technologies, 2007
- [20] Pretorius, J.L. “Design of a Long Conveyor System with Combined Ascending and Descending Sections”, Bulk Solid Handling, Vol 16, No 2, April 1996, pp 195-201
- [21] Gallagher, D. “Low Rolling Resistance for Conveyor Belts”, International Rubber Conference (Oct 2000)

## **AUTHORS' CV**

### **David Kruse**

David Kruse received his B.S. in Engineering Mechanics and Astronautics from the University of Wisconsin, Madison and also has a Masters of Science in Aeronautics and Astronautics from the University of Washington. He is co-owner of Advanced Conveyor Technologies, Inc. His specific interests are in the areas of belt dynamics, data acquisition and field measurements, rubber rheology, and transfer chute design using the discrete element method (DEM). He has developed a wide variety of mining engineering software that is currently in use today.

Advanced Conveyor Technologies, Inc. (AC-Tek)  
19415 594<sup>th</sup> Avenue  
Mankato, Minnesota 56001, U.S.A  
(507) 345-5748  
[www.actek.com](http://www.actek.com)

### **Ryan Lemmon**

Ryan Lemmon received both his Bachelor and Master of Science Mechanical Engineering from the University of Idaho. He is co-owner of Advanced Conveyor Technologies, Inc. His talents include design and analysis of complex conveyor, numerical analysis methods including discrete element method (DEM) and finite element analysis (FEA), data acquisition and field measurements, research and development, and programming.

Advanced Conveyor Technologies, Inc. (AC-Tek)  
3911 East 132 North  
Rigby, ID 83442 U.S.A.  
208) 745-6914  
[www.actek.com](http://www.actek.com)